Hindawi
Advances in Materials Science and Engineering
Volume 2021, Article ID 5526171, 10 pages
https://doi.org/10.1155/2021/5526171

Research Article

Residual Mode Vector-Based Structural Damage Identification with First-Order Modal Information

Shuai Luo, Zhenxin Zhuang, Wei Wang, and Ping Jiang

School of Civil Engineering, Shaoxing University, Shaoxing, Zhejiang 312000, China

Correspondence should be addressed to Ping Jiang; jiangping@usx.edu.cn

Received 15 February 2021; Accepted 16 June 2021; Published 3 July 2021

Academic Editor: Qinglin Guo

Damage identification based on the change of dynamic properties is an issue worthy of attention in structure safety assessment, nevertheless, only a small number of discontinuous members in existing structure are damaged under service condition, and the most remaining members are in good condition. According to this feather, we developed an effective damage location and situation assessment algorithm based on residual mode vector with the first mode information of targeted structure, which utilized the quantitative relationship between first natural modes of global structure with the change of the element stiffness. Firstly, the element damage location is determined with exploitation of the sparseness of element stiffness matrices based on the discontinuity of damaged members. Then, according to the distribution characteristics of the corresponding residual mode vector, the nodal equilibrium equation about the damage parameter is established based on the residual mode vector, and the damage coefficients of structural elements are evaluated with the proposed equations. Two numerical examples are given to verify the proposed algorithm. The results showed that the proposed damage identification method is consistent with the preset damage. It can even accurately identify large-degree damages. The proposed algorithm only required the first-order modal information of the target structures and held few requirements of analysis resource; hence when compared with existing methods, it has obvious advantages for structural damage identification.

1. Introduction

Structural damage identification technology shows its strong vitality in many engineering fields such as civil engineering, mechanical engineering, and aerospace engineering, which has benefited from the combination with modal measurement technology and finite-element analysis [1–3]. Various damage location and detection technologies have been developed based on structural vibration properties. The principle for vibration-based damage identification is that the damage-induced changes in the physical properties of element stiffness will cause detectable changes in system modal properties (natural frequencies and mode shapes).

The investigation of mode eigen values for damage detection is common as the natural frequencies can be conveniently measured from just a few accessible points on the structure [4–7]. However, this method could not detect the subtle damage on structure. Damage detection methods have also been developed for the identification of damage directly based on measured mode shapes or mode shape curvatures [8–10]. A drawback of many mode shape-based methods is the complexity of having measurements from a large number of locations for higher order modal shapes [11–13]. For the purpose of fully utilized mode information, Kaouk and Zimmerman [14–16] defined the residual mode equation for damage detection based on mode information of structure, which can accomplish the dual tasks of determining the damage location and solving the damage situation effectively. This kind of damage detection method has received the widespread attention over the last decade [17–21]. There exists a common obstacle in the aforementioned detection methods, which is to obtain higher order of structural modal shapes. This requirement limits the practical application of the residual mode method. Recently, with the development of high-speed camera and sensitive sensor and vision recognition technology, the modal parameter identification technology of engineering structure has made remarkable progress [22–25]. We can effectively realize the accurate identification of the finite-order natural mode shapes (usually the first order) and natural frequencies (usually the first order) of the structural system. As such, more advanced analysis procedures are required to make the best use of first-order modal information from structural health monitoring.

In this paper, the authors develop a damage detection method originally proposed by Kaouk et al. based on the residual mode equation with only the first order of structure mode information. The residual mode vector is developed based on the residual mode equation for structural element damage detection, in which the relationship between the stiffness matrix of damaged element and first-order mode information is derived from the residual mode equation. Then based on the relationship, the element damage location is determined with exploitation of the sparseness of element stiffness matrices. Finally, according to the distribution characteristics of residual mode vector, a new damage assessment algorithm is proposed.

The presentation of this work is organized as follows: in Section 2, the proposed algorithm based on the residual mode vector is developed. In Section 3, the process of structural damage identification using the established method is introduced numerically in detail with a simple supported beam. Moreover, the source of the accelerated formula is also discussed in detail. A two-story framework example is shown in Section 3.2 to show the feasibility and the superiority of the proposed method. The conclusions of this work are summarized in Section 4.

2. Problem Formulation

2.1. Fundamental Assumptions. In the following theoretical development, the following assumptions are made in damaged structures:

(1) Structural damages only reduce the system stiffness matrix, and structural refined numerical model has been developed before damage occurrence.

(2) It is assumed that the effect of damage on the mass properties of the structure is negligible, and we assume that the structure under consideration is undamped.

(3) The crack-induced structural member damage is not continuous in the finite-element model, this is reasonable in the previous study [26–29], and furthermore we could change the scale of element size in the numerical model.

2.2. Theoretical Development. One basic approach to obtain a qualitative feel for the effect of the damage on an individual mode is to monitor the change in mode information between the damaged structures and the undamaged structures. With the above assumptions, considering an initial design, the first-mode eigen equation of an n-DOF finite-element model of the undamaged structure exists and is given as

$$\lambda_1 \mathbf{M}\phi_1 = \mathbf{K}\phi_1, \quad (1)$$

where λ_1 and ϕ_1 are the first-mode eigen value and corresponding eigenvector separately and $\mathbf{M}$ and $\mathbf{K}$ are the $n \times n$ analytical mass and stiffness matrices. In this paper, only the first-order modal information of the system will be used to identify the damage location and damage situation, and this is also the important motivation for conducting this research. Let $\Delta\mathbf{K}$ be the exact perturbation matrices that reflect the nature of the structural damage. Thus, the exact perturbation matrices are sparse matrices with the nonzero elements reflecting the state of damage. The eigen equation for the damaged structure is then

$$\lambda_{1\mathrm{d}} \mathbf{M}\phi_{1\mathbf{d}} = (\mathbf{K} - \Delta\mathbf{K})\phi_{1\mathbf{d}}, \quad (2)$$

where λ_{1d} and $\phi_{1\mathbf{d}}$ are the first-mode eigen value and corresponding eigenvector measured precisely, as the first-order modal parameters of structures are the most easily obtained dynamic information in experimental process. $\Delta\mathbf{K}$ is the $n \times n$ analytical mass and stiffness matrices:

$$\Delta\mathbf{K} = \sum_m \alpha_m \mathbf{K}_\mathbf{m}, \quad (3)$$

where α_m is a scalar denoting the damage extent corresponding to the m-th element and the $\Delta\mathbf{K}$ matrices represent the effect of damage on the structural property matrices. Thus, the exact damage matrices are sparse matrices with the nonzero elements reflecting the state of damage. Now equation (2) can be rewritten in the dynamic residual form:

$$\Delta\mathbf{K}\phi_{1\mathbf{d}} = (\mathbf{K} - \lambda_{1\mathrm{d}}\mathbf{M})\phi_{1\mathbf{d}} = \mathbf{D}, \quad (4)$$

where $\mathbf{D}$ is the defined residual mode vector related to the first mode about the damaged system, and it could be depicted as

$$\mathbf{D} = [\, d_1, \; d_2, \; \cdots \; d_n \,]^T, \quad (5)$$

where superscript T means transpose, and the same below, the proposed residual mode vector is $n \times 1$ column vector. Then the location of damage element could be easily processed based on the distribute regulation of the proposed residual mode vector. Sort the elements in residual mode vector in absolute descending order, and then one can easily find that there is a great deal of differences: The amplitude of d_i in the proposed residual mode vector corresponding to the damaged element is much larger than that of the undamaged element; even, the elements in the proposed residual mode vector corresponding to undamaged element tends to 0, which could be used as the basis of filtering in the analysis process.

Obviously, equation (4) is composed of n equilibrium equations at nodes; based on the assumption that there is only one element damaged at each node, for the node location of the damage element, the stiffness of the independent damage element is strictly proportional to the right-hand side of equation (4), and its ratio is the damage coefficient to be calculated. Based on this principle, the damage situation could be evaluated quantitatively.

In the end, this section summarizes the key steps as follows:

Step 1: calculating the residual mode vector

For the target structure, calculate residual mode vector by substituting the experimental results of first-order modal information $\lambda_{1\,d}$ and $\phi_{\mathbf{1d}}$ into equation (4).

Step 2: locating the damage element in structure and filter

Arrange the elements in the residual mode vector in the descending order of their absolute values. Divide the previous element by the next, and the last damage element is where the result tends to infinity, so as to locate the damage element; then the element in residual mode vector corresponding to the undamaged unit after positioning is artificially set to 0 to realize filtering.

Step 3: Verifying the results of location identification

List the elements in residual mode vector after filtering according to their corresponding structural elements. Divide the elements in residual mode vector corresponding to the symmetrical node in the element, and the result whose quotient is −1 is the damaged component, so as to *verify* the results of location identification in Step 3, and prepare a new list for identification of the damage situation quantitatively.

Step 4: Evaluating the damage coefficient

Take out the stiffness matrix of the damage element after positioning, establish the balance equation on the node position one by one according to the damage element code, and complete the damage identification by evaluating the damage coefficient of the balance equation.

To conclude this section, the process of the proposed vibration measurements using only first-order modal information mainly involves two key influence factors: precise of first mode information and sparse of element stiffness matrix. More details are explained in the following numerical examples.

3. Numerical Examples

3.1. Simply Supported Beam. A 12-element simply supported beam used in this example shown in Figure 1 is employed to exercise the proposed method. The basic parameters of the beam are as follows: Young's modulus $E = 200$ GPa, density $\rho = 7.8\times10^3\ \text{kg/m}^3$, length of each element $L = 0.1$ m, and cross-sectional area $A = 2.5\times10^{-3}\ \text{m}^2$. The finite-element model of the structure has 26 degrees of freedom.

Let the beam element stiffness matrix in local coordination can be represented as

$$\mathbf{K_e} = \frac{EI}{L^3}\begin{bmatrix} 12 & 6L & -12 & 6L \\ 6L & 4L^2 & -6L & 2L^2 \\ -12 & -6L & 12 & -6L \\ 6L & 2L^2 & -6L & 4L^2 \end{bmatrix}. \tag{6}$$

The corresponding element mass matrix is

$$\mathbf{M_e} = \frac{\rho A}{420}\begin{bmatrix} 156L & 22L^2 & 54L & -13L \\ 22L^2 & 4L^3 & 13L^2 & -3L^3 \\ 54L & 13L^2 & 156L & -22L^2 \\ -13L & -3L^3 & -22L^2 & 4L^3 \end{bmatrix}. \tag{7}$$

The local coordinate of each element is consistent with the global coordination; hence, the coordination transformation is unnecessary; the element stiffness matrix represented by all element node displacements in the global coordinate system is derived directly as equation (1). The deformation vector of each node in the overall coordinate system is set as

$$\mathbf{V} = [\, v_1 \ \ \theta_1 \ \ v_2 \ \ \theta_2 \ \ \ldots \ \ v_{12} \ \ \theta_{12} \ \ v_{13} \ \ \theta_{13} \,]^{\mathrm{T}}. \tag{8}$$

Take element 3, for example, the deformation vector corresponding to K_3^e can be expressed as

$$\mathbf{V_{3e}} = [\, v_3 \ \ \theta_3 \ \ v_4 \ \ \theta_4 \,]^{\mathrm{T}}. \tag{9}$$

According to the relationship of the deformation vector between local and global coordination, the element matrix under global coordination system is given by

$$\mathbf{V_{3e}} = \mathbf{SV}, \tag{10}$$

where the connective matrix $\mathbf{S}$ is 4×26, the element in row 1 and column 5 of $\mathbf{S}$ is 1; the element in row 2 and column 6 of $\mathbf{S}$ is 1; the element in row 3 and column 7 of $\mathbf{S}$ is 1; the element in row 4 and column 8 of $\mathbf{S}$ is 1; and the rest of the elements of $\mathbf{S}$ is 0. The connective matrix $\mathbf{S}$ can be expressed as

$$\mathbf{S} = \begin{bmatrix} 0 & \ldots & 0 & 1 & 0 & 0 & 0 & 0 & \ldots & 0 \\ 0 & \ldots & 0 & 0 & 1 & 0 & 0 & 0 & \ldots & 0 \\ 0 & \ldots & 0 & 0 & 0 & 1 & 0 & 0 & \ldots & 0 \\ 0 & \ldots & 0 & 0 & 0 & 0 & 1 & 0 & \ldots & 0 \end{bmatrix}_{4\times26}. \tag{11}$$

The elastic strain energy of element 3 can be derived based on the energy theorem as

$$\mathbf{U}_3 = \mathbf{V}_{3\mathbf{e}}^{\mathbf{T}}\mathbf{K}_3^{\mathbf{e}}\mathbf{V}_{3\mathbf{e}}. \tag{12}$$

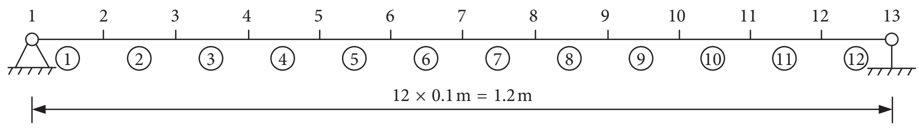

Figure 1: The finite element model of simply supported beam.

Substitute equation (10) into equation (12), we can get

$$\begin{aligned}\mathbf{U}_3 &= \mathbf{V}^{\mathrm{T}}\mathbf{S}_3^{\mathrm{T}}\mathbf{K}_3^{\mathbf{e}}\mathbf{S}_3,\\ \mathbf{V} &= \mathbf{V}^{\mathrm{T}}\mathbf{K}_3^{\mathbf{g}}\mathbf{V}.\end{aligned} \tag{13}$$

Hence, the element stiffness matrix of element 3 under the global coordination can be expressed as

$$K_3^g = S_3^T K_3^e S_3. \tag{14}$$

The element stiffness matrix under the global coordination could be derived similarly; then the whole stiffness matrix of the beam is obtained as

$$\mathbf{K} = \sum_{\mathrm{i}=1}^{12} (1-\alpha_i)\mathbf{K}_{\mathbf{i}}^{\mathbf{g}}, \tag{15}$$

where $\alpha_i\,(0 \le \alpha_i < 1)$ is taken as an unknown variable expressed as a damage coefficient of the corresponding element i, and for undamaged theoretical model, these damage coefficients are all zeros.

With the same procedure, the whole mass matrix **M** could be derived; then the modal equilibrium equation of the undamaged structural system shown in equation (1) is obtained, and the damage identification of the structure will be studied with this equation. Obviously, for single element in the global system, its element stiffness matrix is sparse, which provides important clues for damage identification.

For the damaged beam, preset the damage coefficient artificially as $\alpha_2 = 0.15$, $\alpha_4 = 0.6$, $\alpha_8 = 0.13$, and $\alpha_{10} = 0.3$, and the rest elements are intact. Figure 2 shows the measured first eigenvector ϕ_{1d} of the damaged system, with which the corresponding eigen value $\lambda_{1d} = 1033.5$.

Then the first-order eigen value λ_{1d} and eigenvector $\boldsymbol{\phi}_{\mathbf{1d}}$ of the damaged beam are substituted into equation (4) to obtain the residual mode vector. Figure 3 shows the distribution diagram of residual mode vector obtained from equation (4). The vector is numbered according to the degrees of freedom (abscissa) of the element. Since each element is statically self-balanced according to mode shape, the residual mode vector corresponding to each element is symmetric about the x-axis; hence the sum is 0.

The first purpose in this analysis is to determine the location of the damage. Arrange the absolute value of the obtained residual mode vector from large to small in accordance with Step 2. It should be noted that for the absolute value of residual mode vector from large to small, the number of the corresponding abscissa in Figure 3 of each ordered element of residual mode vector must be marked first before the sorting, which is important for the subsequent damage detection work. Then, according to Step 3, obtain the location map of damage element as shown in Figure 4. The abscissa is the number of degrees of freedom of

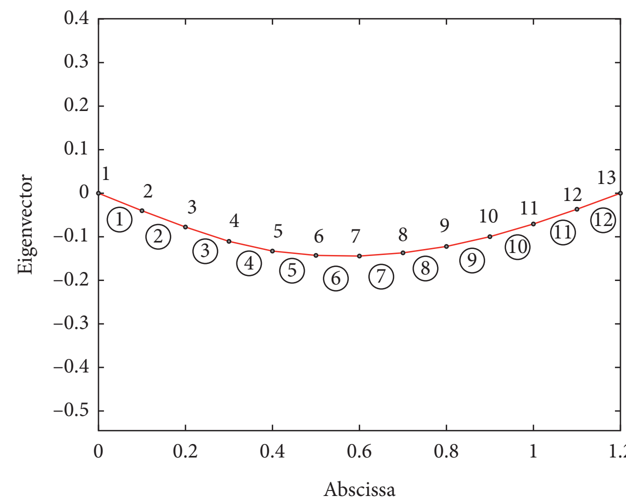

Figure 2: The measured first modal eigenvector.

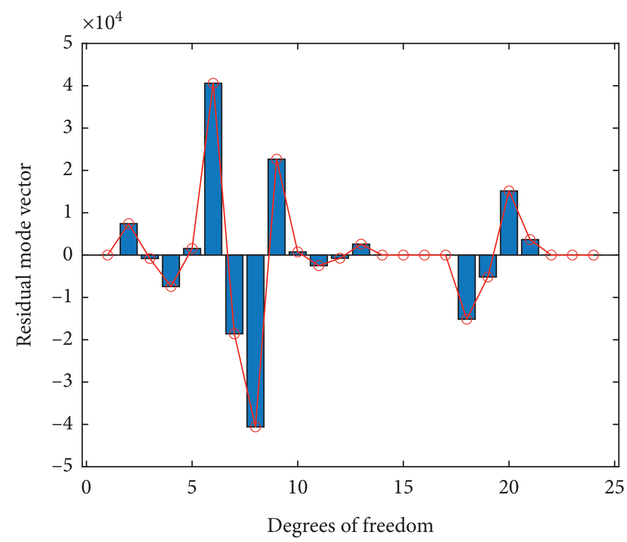

Figure 3: The distribution diagram of residual mode vector.

the unit, the ordinate is the ratio, the peak position in the figure is 16, and each unit corresponds to four degrees of freedom. Therefore, it is clear that four damaged elements are present in the simply supported beam, which is consistent with the presetting.

The next step of this analysis is to verify the location of the structural damage. Referring to Step 4, the residual mode vector of the corresponding elements is arranged in Table 1 according to the node code of each element, and the first variable of each element is divided by the third variable. The element whose quotient equals minus is the damage

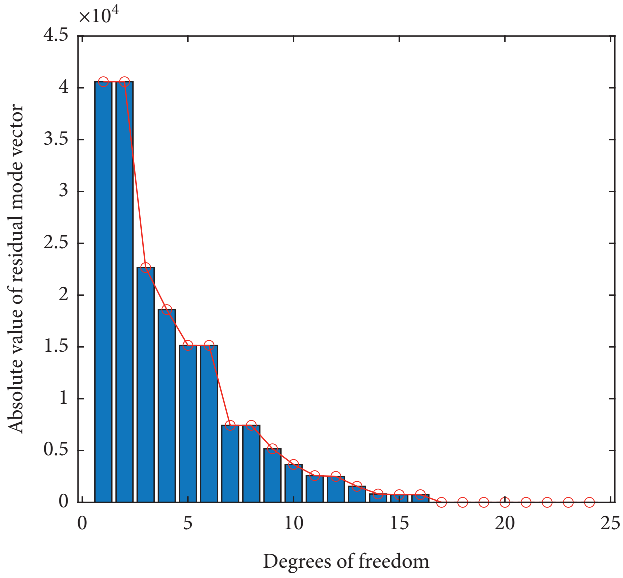

FIGURE 4: The location map of the damage element.

component, so as to verify the results of damage element location in the third step. Obviously, the results of damage location are consistent with the presetting, which verifies the results of Step 3 again.

The last step of this analysis is to determine the extent of structural damage with the damage location according to Step 4. Take out the stiffness matrix of the element after damage location, and calculate $\mathbf{K_m}\phi_{\mathbf{1d}}$ in the left-hand side of equation (4), respectively, as shown in Figure 5. At the same time, take out the residual mode vector of the damage element located in Table 1, and express it in Figure 5. By comparison, for the given damage element, the elements in D_m are proportional to the product vector of the element stiffness matrix $\mathbf{K_m}$ and the first-mode shape $\phi_{\mathbf{1d}}$, and the ratio is the damage degree α_m.

As the located elements, 2, 4, 6, and 10 are discontinuous members in this study, and the following formula can be used to solve the damage coefficient:

$$\boldsymbol{\alpha}_{\mathbf{m}}\mathbf{K_m}\phi_{\mathbf{1d}} = \mathbf{D_m}. \tag{16}$$

Finally, the damage parameters obtained are listed in Table 2. From the table, it can be easily seen that the results calculated by this method are accurate solutions with Equation (16) which reflects the advantage of the proposed algorithm.

The results in this section indicate that only the first mode of the structure needs to be provided by the algorithm proposed in this paper. Compared with the commonly used identification methods, the experimental requirements were not strict. Therefore, the proposed method has obvious advantages for structural damage identification. This paper will continue to use an example of a frame structure to further verify the results.

3.2. Two-Story Frame Structure. The second example is a two-story frame structure as shown in Figure 6. This frame was modeled with 24 equal elements of 0.2 m in length. Every node has 3 DOFs, an axial displacement, a transverse displacement, and a rotation. The properties of this structure are as follows: cross-sectional area $A = 0.0336\ \text{m}^2$; moment of inertia $I = 1.6128 \times 10^{-4}\ \text{m}^4$; Young's modulus $E = 200\ \text{GPa}$; and density $\rho = 2500\ \text{kg/m}^3$.

The stiffness matrix of frame element considering axial deformation can be expressed as

$$\mathbf{K_{ef}} = \frac{EA}{L}\begin{bmatrix} 1 & 0 & 0 & -1 & 0 & 0 \\ 0 & 0 & 0 & 0 & 0 & 0 \\ 0 & 0 & 0 & 0 & 0 & 0 \\ -1 & 0 & 0 & 1 & 0 & 0 \\ 0 & 0 & 0 & 0 & 0 & 0 \\ 0 & 0 & 0 & 0 & 0 & 0 \end{bmatrix} + \frac{EI}{L^3}\begin{bmatrix} 0 & 0 & 0 & 0 & 0 & 0 \\ 0 & 12 & 6L & 0 & -12 & 6L \\ 0 & 6L & 4L^2 & 0 & -6L & 2L^2 \\ 0 & 0 & 0 & 1 & 0 & 0 \\ 0 & -12 & -6L & 0 & 12 & -6L \\ 0 & 6L & 2L^2 & 0 & -6L & 4L^2 \end{bmatrix}. \tag{17}$$

The corresponding element mass matrix is

$$\mathbf{M_{ef}} = \frac{\rho AL}{6}\begin{bmatrix} 2 & 0 & 0 & 1 & 0 & 0 \\ 0 & 0 & 0 & 0 & 0 & 0 \\ 0 & 0 & 0 & 0 & 0 & 0 \\ 1 & 0 & 0 & 2 & 0 & 0 \\ 0 & 0 & 0 & 0 & 0 & 0 \\ 0 & 0 & 0 & 0 & 0 & 0 \end{bmatrix} + \frac{\rho AL}{420}\begin{bmatrix} 0 & 0 & 0 & 0 & 0 & 0 \\ 0 & 156 & 22L & 0 & 54 & -13L \\ 0 & 22L & 4 & 0 & 13L & -3L^2 \\ 1 & 0 & 0 & 0 & 0 & 0 \\ 0 & 54 & 13L & 0 & 156 & -22L \\ 0 & -13L & -3L^2 & 0 & -22L & 4L^2 \end{bmatrix}. \tag{18}$$

Table 1: Residual mode vector according to elements.

Element no.	1	2	3	4	5	6	7	8	9	10	11	12
Residual	0	7431.3	−7431.3	40591.4	−40591.4	743.4	−743.4	0	0.0	−15147.5	15147.5	0
Force	0	−805.2	1548.4	−18598.0	22657.1	−2504.3	2578.6	0	0.0	−5172.5	3657.8	0
Vector	7431.3	−7431.3	40591.4	−40591.4	743.4	−743.4	0.0	0	−15147.5	15147.5	0.0	0
Residual mode vector	−805.2	1548.4	−18598.0	22657.1	−2504.3	2578.6	0.0	0	−5172.5	3657.8	0.0	0

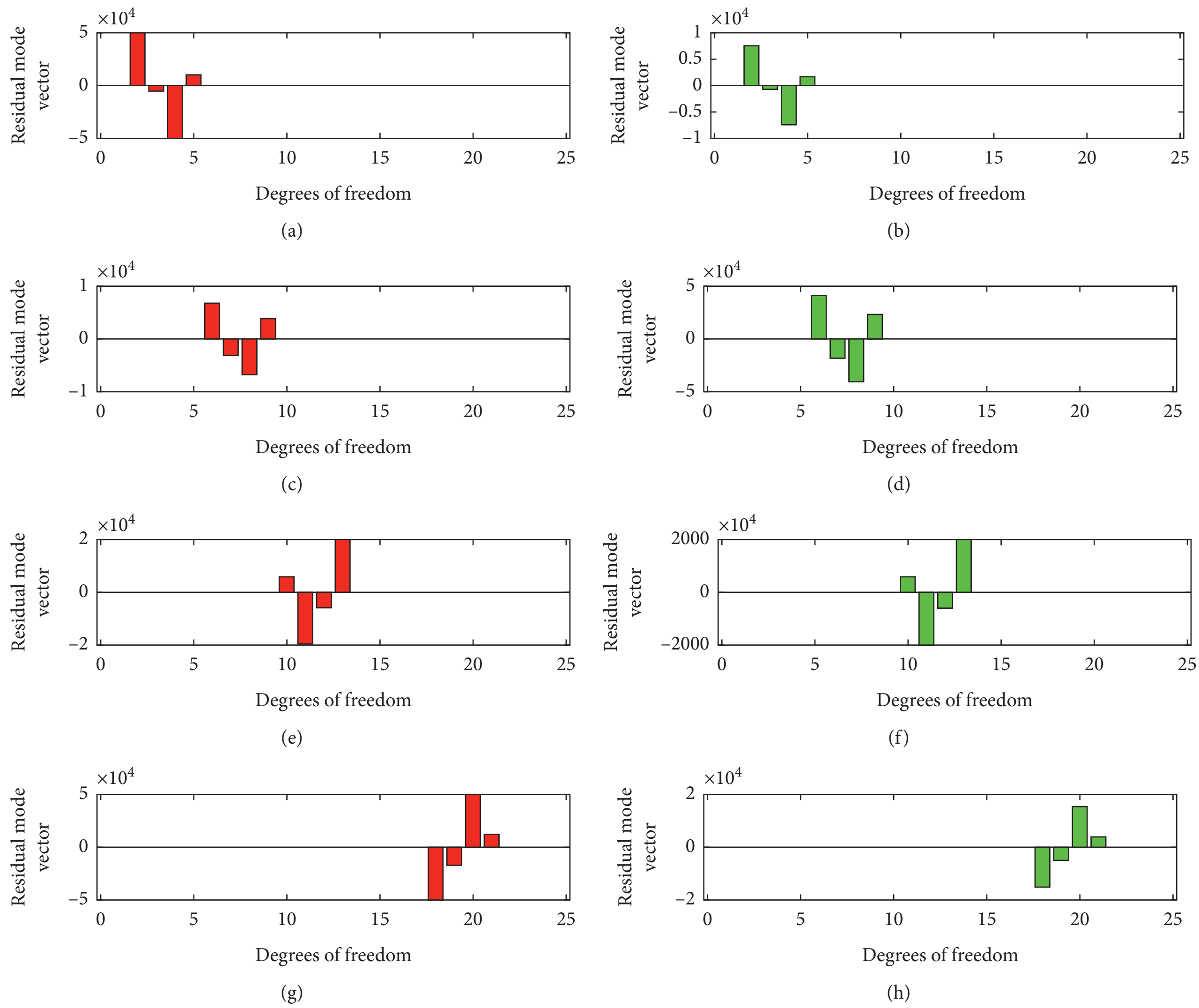

Figure 5: Residual mode vector according to damage location.

Table 2: The evaluated damage parameters.

Element no 2			Element no 4			Element no 6			Element no 10		
$\mathbf{K}_2\phi_{\mathbf{1d}}$	$\mathbf{D}_2$	α_2	$\mathbf{K}_4\phi_{\mathbf{1d}}$	$\mathbf{D}_4$	α_4	$\mathbf{K}_6\phi_{\mathbf{1d}}$	$\mathbf{D}_6$	α_6	$\mathbf{K}_{10}\phi_{\mathbf{1d}}$	$\mathbf{D}_{10}$	α_{10}
7431.2	49541.8	0.15	40591.3	67652.2	0.6	743.3	5718.2	0.13	−15147.5	−50491.6	0.3
−805.2	−5368.2	0.15	−18598	−30996.6	0.6	−2504.2	−19263.6	0.13	−5172.5	−17241.8	0.3
−7431.2	−49541.9	0.15	−40591.4	−67652.3	0.6	−743.3	−5718.2	0.13	15147.4	50491.6	0.3
1548.3	10322.4	0.15	22657.1	37761.8	0.6	2578.6	19835.4	0.13	3657.7	12192.6	0.3

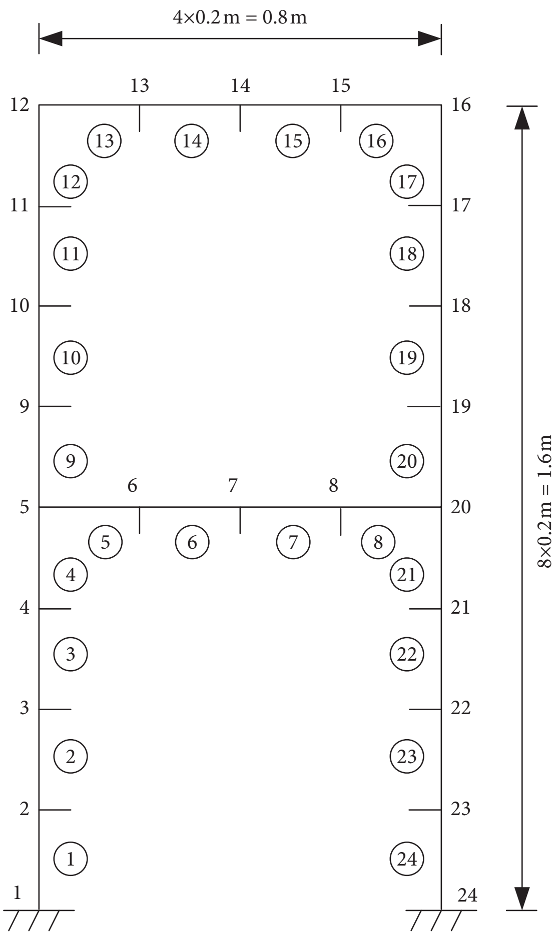

Figure 6: Two-story frame structure.

Taking element 3 as an example, suppose the element stiffness matrix in the local coordinate system is $\mathbf{K}_{\mathbf{3ef}}$, and the displacement vector in the local coordinate system can be expressed as

$$\mathbf{V}_{\mathbf{3ef}} = [\ u_{3a} \ \ v_{3a} \ \ \theta_{3a} \ \ \ u_{4b} \ \ v_{4b} \ \ \theta_{4b}\ ]^{\mathrm{T}}. \tag{19}$$

According to the energy theorem, the elastic strain energy of the third element is known to be

$$\mathbf{U}_{\mathbf{3ef}} = \mathbf{V}^{\mathbf{T}}_{\mathbf{3ef}} \mathbf{K}_{\mathbf{3ef}} \mathbf{V}_{\mathbf{3ef}}. \tag{20}$$

The relationship between the deformation of element component 3 in the local coordination and the global coordination needs to transform in the numerical model as the local coordinate of each element is inconsistent with the global coordination, which is different from the simply supported beam example.

The displacement vector in the global coordinate system can be expressed as

$$\mathbf{V}_{\mathbf{3g}} = [\ u_3 \ \ v_3 \ \ \theta_3 \ \ \ u_4 \ \ v_4 \ \ \theta_4\ ]^{\mathrm{T}}. \tag{21}$$

Then the mapping relationship between local coordinates and global coordinates can be found as [30]

$$\mathbf{V}_{\mathbf{3g}} = \mathbf{P}\mathbf{V}_{\mathbf{3ef}}, \tag{22}$$

where the matrix P representing the mapping relationship is a 6×6 matrix as

$$\mathrm{P}_3 = \begin{bmatrix} \cos(\alpha_3) & -\sin) & 0 & 0 & 0 & 0 \\ \sin(\alpha_3) & \cos(\alpha_3) & 0 & 0 & 0 & 0 \\ 0 & 0 & 1 & 0 & 0 & 0 \\ 0 & 0 & 0 & \cos(\alpha_3) & -\sin(\alpha_3) & 0 \\ 0 & 0 & 0 & \sin(\alpha_3) & \cos(\alpha_3) & 0 \\ 0 & 0 & 0 & 0 & 0 & 1 \end{bmatrix}, \tag{23}$$

where a_3 is the rotation angle of element 3 in the frame, and obviously the angle is $\pi/2$. By substituting equation (22) into equation (20), the following equations can be obtained by energy theorem as

$$\mathbf{U}_{\mathbf{3ef}} = \mathbf{V}^{\mathbf{T}}_{\mathbf{3g}} \left(\mathbf{P}_3^{-1}\right)^{\mathbf{T}} \mathbf{K}_{\mathbf{3ef}} \mathbf{P}_3^{-1} \mathbf{V}_{\mathbf{3g}}. \tag{24}$$

Thus, the stiffness matrix of element 3 under the global coordination can be derived as

$$\mathbf{K}_{\mathbf{3eg}} = \left(\mathbf{P}_3^{-1}\right)^{\mathbf{T}} \mathbf{K}_{\mathbf{3ef}} \mathbf{P}_3^{-1}. \tag{25}$$

Furthermore, the stiffness matrix of element 3 represented by the overall displacement vector of the frame structure in the global coordination is derived directly. The deformation vector of each node in the global coordination is set as

$$\mathbf{V}_{\mathbf{f}} = [\ u_1 \ \ v_1 \ \ \theta_1 \ \ \ldots \ u_{24} \ \ v_{24} \ \ \theta_{24}\ ]^{\mathrm{T}}. \tag{26}$$

As the simple supported beam model in example 1, the connective relationship between the element displacement vector and the overall displacement vector is given by

$$\mathbf{V}_{\mathbf{3g}} = \mathbf{S}\mathbf{V}_{\mathbf{f}}, \tag{27}$$

where the connective matrix $\mathbf{S}$ is 6×72. According to the corresponding relationship of $\mathbf{V}_{\mathbf{f}}$ and $\mathbf{V}_{\mathbf{3g}}$, the connective matrix $\mathbf{S}_\mathbf{3}$ can be expressed as

$$\mathbf{S}_3 = \begin{bmatrix} 0 & \ldots & 0 & 1 & 0 & 0 & 0 & 0 & 0 & 0 & \ldots & 0 \\ 0 & \ldots & 0 & 0 & 1 & 0 & 0 & 0 & 0 & 0 & \ldots & 0 \\ 0 & \ldots & 0 & 0 & 0 & 1 & 0 & 0 & 0 & 0 & \ldots & 0 \\ 0 & \ldots & 0 & 0 & 0 & 0 & 1 & 0 & 0 & 0 & \ldots & 0 \\ 0 & \ldots & 0 & 0 & 0 & 0 & 0 & 1 & 0 & 0 & \ldots & 0 \\ 0 & \ldots & 0 & 0 & 0 & 0 & 0 & 0 & 1 & 0 & \ldots & 0 \end{bmatrix}, \tag{28}$$

where the element in row 1 and column 7 of $\mathbf{S}_\mathbf{3}$ is 1; the element in row 2 and column 8 of $\mathbf{S}_\mathbf{3}$ is 1; the element in row 3 and column 9 of $\mathbf{S}_\mathbf{3}$ is 1; the element in row 4 and column 10 of $\mathbf{S}_\mathbf{3}$ is 1; the element in row 5 and column 11 of $\mathbf{S}_\mathbf{3}$ is 1; the element in row 6 and column 12 of $\mathbf{S}_\mathbf{3}$ is 1; and rest of the elements of $\mathbf{S}$ is zero. Substitute equation (27) into equation (24), the strain energy can be deduced as

$$\begin{aligned} \mathbf{U}_{\mathbf{3e}} &= \mathbf{V}^{\mathbf{T}} \mathbf{S}_3^{\mathbf{T}} \mathbf{K}_{\mathbf{3eg}}, \\ \mathbf{S}_3 \mathbf{V} &= \mathbf{V}^{\mathbf{T}} \mathbf{K}_3^{\mathbf{g}} \mathbf{V}. \end{aligned} \tag{29}$$

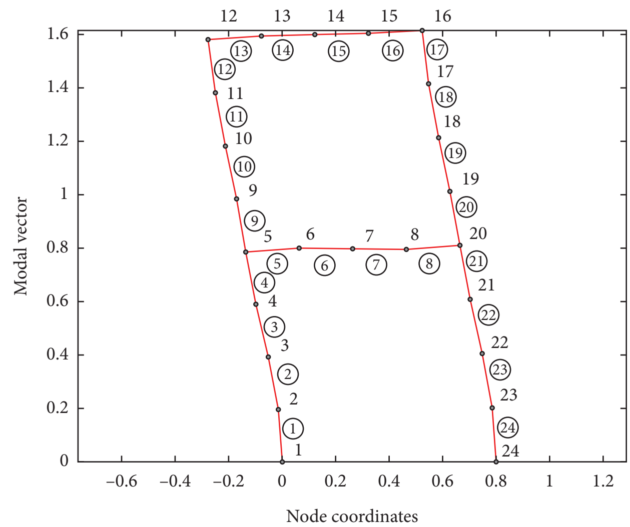

Figure 7: The measured first eigenvector of the frame structure.

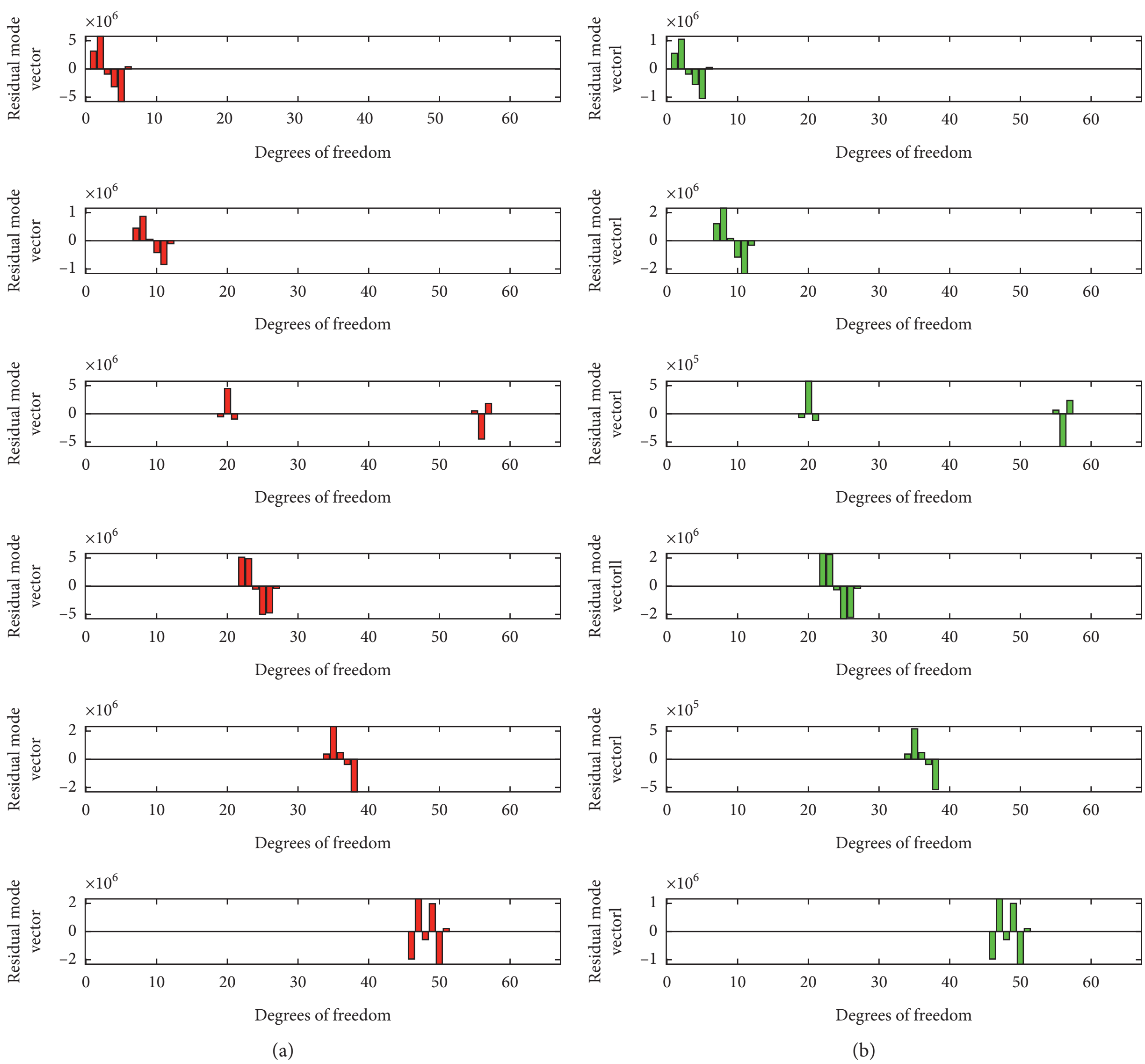

Figure 8: Component schematic diagram: (a) the amount of $K_m\phi_{1\,d}$. (b) The residual mode vector of the damage element.

Table. 3: The evaluated damage parameters.

Element no 2		Element no 4		Element no 8		Element no 10		Element no 14		Element no 18	
$K_2\phi_{1\,d}$	D_2	$K_4\phi_{1\,d}$	D_4	$K_8\phi_{1\,d}$	D_8	$K_{10}\phi_{1\,d}$	D_{10}	$K_{14}\phi_{1\,d}$	D_{14}	$K_{18}\phi_{1\,d}$	D_{18}
3211025	481653.7	3581720	1074516	−440108	−57214	4332774	2599664	321187.5	73873.12	−2235587	−894235
5930163	889524.4	7166890	2150067	3836174	498702.6	4061953	2437172	2002432	460559.4	2652865	1061146
−993756	−149063	330389.7	99116.92	−765979	−99577.2	−524497	−314698	419546.6	96495.72	−681415	−272566
−3211025	−481654	−3581720	−1074516	440108	57214.04	−4332774	−2599664	−321187	−73873.1	2235587	894234.8
−5930163	−889524	−7166890	−2150067	−3836174	−498703	−4061953	−2437172	−2002432	−460559	−2652865	−1061146
351551.4	52732.71	−1046734	−314020	1533214	199317.8	−342058	−205235	−19060.2	−4383.84	234297.8	93719.13
$\alpha_2 = 0.15$		$\alpha_4 = 0.3$		$\alpha_8 = 0.13$		$\alpha_{10} = 0.6$		$\alpha_{14} = 0.23$		$\alpha_{18} = 0.4$	

Substitute equation (25) into equation (29), then the stiffness matrix of element 3 under the global coordination can be expressed by the overall displacement vector as

$$\mathbf{K}_3^{\mathbf{g}} = \mathbf{S}_3^{\mathbf{T}}\left(\mathbf{P}_3^{-1}\right)^{\mathbf{T}}\mathbf{K}_{3\mathbf{ef}}\mathbf{P}_3^{-1}\mathbf{S}_3. \tag{30}$$

The element stiffness matrix of the rest elements in global coordination can be obtained by the same procedure. Obviously, for each single element component, the stiffness matrix is a sparse matrix, and its sparse property is the key foundation of the proposed damage identification method.

As the next step is establishing the whole stiffness matrix of the structure system in global matrix, the element stiffness matrix under the global coordination could be derived similarly, and the whole stiffness matrix of the frame structure can be expressed as

$$\mathbf{K} = \sum_{i=1}^{24}\left(1 - \alpha_i\right)\mathbf{K}_{\mathbf{i}}^{\mathbf{g}}, \tag{31}$$

where $\alpha_i\,(0 \leq \alpha_i < 1)$ is taken as an unknown variable expressed as the damage coefficient corresponding to element i, and for undamaged theoretical model these damage coefficients are all zeros. With the same procedure, the whole mass matrix $\mathbf{M}$ could be derived by the element mass matrix in equation (18), then the modal equilibrium equation of undamaged structural system shown in formula (1) is obtained, and the damage identification of the structure could be studied based on it. The stiffness of the single element in the global system is spare, whose nodal points are coupled. Thus, it would provide important clues for damage identification obviously.

For the damaged frame structure, we could preset the damage coefficients artificially as $\alpha_2 = 0.15$, $\alpha_4 = 0.3$, $\alpha_8 = 0.13$, $\alpha_{10} = 0.6$, $\alpha_{14} = 0.23$, and $\alpha_{18} = 0.4$, and the rest elements are intact. Figure 7 shows the measured first eigenvector $\boldsymbol{\phi}_{\mathbf{1d}}$ of the damaged system, with which the corresponding eigen value $\lambda_{1d} = 58814.7$. The same operation could be operated for damage identification of frame structures, which takes an example of the previous proposed beam.

The first-order eigen value $\lambda_{1\mathrm{d}}$ and eigenvector $\phi_{\mathbf{1d}}$ of the damaged beam are substituted into equation (4) to obtain the residual mode vector. Take out the stiffness matrix of the element after damage location, and calculate the amount of $\mathbf{K}_{\mathbf{m}}\phi_{\mathbf{1d}}$ in the left-hand side of equation (4), respectively, as shown in Figure 8(a) and take out the residual mode vector of the damage element and express it in Figure 8(b). By comparison, for the given damage element, the element value in residual mode vector is proportional to the product vector of the element stiffness matrix $\mathbf{K}_{\mathbf{m}}$ and the first mode shape $\phi_{\mathbf{1d}}$, and the ratio is the damage degree α_m.

The damage coefficients can be evaluated by equation (16). Table 3 shows the amount of $\mathbf{K}_{\mathbf{m}}\phi_{\mathbf{1d}}$ in the left-hand side of equation (16), and the residual mode vector corresponding to the located damage members of the frame structure. From the table, it can be seen that the results calculated by this method are accurately the same as those preset, which further proves the reliability of this proposed method.

According to the solution results of the two numerical examples, only the first-order mode of the structure needs to be measured by the method developed in this paper. Compared with the commonly used identification method, the experimental requirements are not strict, and the measured results are accurate solutions, so the solution results are better than the approximate methods such as sensitivity method, which is worth popularizing. Therefore this research develops a new strategy of structural damage identification based on first-order mode and opens up a new way for structural damage identification based on the dynamic test.

4. Conclusions

This study presents an accurate algorithm for structural damage identification and location based on the measured first-order modal information of structure according to the sparse characteristics of the element stiffness matrix. The only location results required in determining the damage in the first-order modal equilibrium equation is the common residual mode vector whose nonzero elements are corresponding to the damaged member in the structure system. Finally based on the location results, the mechanical balance equation of the residual deformation of the located element is formulated for determining the damage extent. The proposed method has the advantages of low calculation resource requirement, fast positioning speed, and high recognition accuracy. As the higher order modal information could not be acquired sufficiently with the current technology, the process of computing the extent of structural damage using the proposed algorithm is shown to be computationally attractive and hence suitable for large-scale problems.

Data Availability

The data used to support the findings of this study are available from the corresponding author upon request.

Conflicts of Interest

The authors declare that they have no conflicts of interest.

References

[1] S. W. Doebling, C. R. Farrar, and M. B. Prime, "A summary review of vibration-based damage identification methods," *The Shock and Vibration Digest*, vol. 30, no. 2, pp. 91–105, 1998.

[2] W. Wei Fan and P. Z. Pizhong Qiao, "Vibration-based damage identification methods: a review and comparative study," *Structural Health Monitoring*, vol. 10, no. 1, pp. 83–111, 2011.

[3] A. D. Dimarogonas, "Vibration of cracked structures: a state of the art review," *Engineering Fracture Mechanics*, vol. 55, no. 5, pp. 831–857, 1996.

[4] A. Mehrisadat Makki, G. Linlin, K. Kamyar, Z. Yincai, H. Bruce, and D. Zheyuan, "Non-contact structural health monitoring of a cable-stayed bridge: case study," *Structure and Infrastructure Engineering*, vol. 15, pp. 1119–1136, 2019.

[5] Z. Li, M. Q. Feng, L. Luo, D. Feng, and X. Xu, "Statistical analysis of modal parameters of a suspension bridge based on Bayesian spectral density approach and SHM data," *Mechanical Systems and Signal Processing*, vol. 98, pp. 352–367, 2018.

[6] D. Ribeiro, R. Calçada, R. Delgado, M. Brehm, and V. Zabel, "Finite element model updating of a bowstring-arch railway bridge based on experimental modal parameters," *Engineering Structures*, vol. 40, pp. 413–435, 2012.

[7] W. Di and S. S. Law, "Eigen-parameter decomposition of element matrices for structural damage detection," *Engineering Structures*, vol. 29, no. 4, pp. 519–528, 2007.

[8] Y. B. Yang, B. Zhang, Y. Qian, and Y. Wu, "Contact-point response for modal identification of bridges by a moving test vehicle," *International Journal of Structural Stability and Dynamics*, vol. 18, no. 5, Article ID 1850073, 2018.

[9] Y. Oshima, K. Yamamoto, and K. Sugiura, "Damage assessment of a bridge based on mode shapes estimated by responses of passing vehicles," *Smart Structures and Systems*, vol. 13, no. 5, pp. 731–753, 2014.

[10] Y. Zhang, S. T. Lie, and Z. Xiang, "Damage detection method based on operating deflection shape curvature extracted from dynamic response of a passing vehicle," *Mechanical Systems and Signal Processing*, vol. 35, no. 1-2, pp. 238–254, 2013.

[11] A. Malekjafarian and E. J. Obrien, "Identification of bridge mode shapes using short time frequency domain decomposition of the responses measured in a passing vehicle," *Engineering Structures*, vol. 81, pp. 386–397, 2014.

[12] M. Frizzarin, M. Q. Feng, P. Franchetti, S. Soyoz, and C. Modena, "Damage detection based on damping analysis of ambient vibration data," *Structural Control and Health Monitoring*, vol. 17, pp. 368–385, 2010.

[13] M. Brehm, V. Zabel, and C. Bucher, "An automatic mode pairing strategy using an enhanced modal assurance criterion based on modal strain energies," *Journal of Sound and Vibration*, vol. 329, no. 25, pp. 5375–5392, 2010.

[14] M. Kaouk and D. C. Zimmerman, "Structural damage assessment using a generalized minimum rank perturbation theory," *AIAA Journal*, vol. 32, no. 4, pp. 836–842, 1994.

[15] D. C. Zimmerman and M. Kaouk, "Structural damage detection using a minimum rank update theory," *Journal of Vibration and Acoustics*, vol. 116, no. 2, pp. 222–231, 1994.

[16] S. W. Doebling, "Minimum-rank optimal update of elemental stiffness parameters for structural damage identification," *AIAA Journal*, vol. 34, no. 12, pp. 2615–2621, 1996.

[17] Q. Yang, C. Wang, N. Li, S. Luo, and W. Wang, "Model-free method for damage localization of grid structure," *Applied Sciences*, vol. 9, no. 16, p. 3252, 2019.

[18] B. Zhang, Y. Qian, Y. Wu, and Y. B. Yang, "An effective means for damage detection of bridges using the contact-point response of a moving test vehicle," *Journal of Sound and Vibration*, vol. 419, pp. 158–172, 2018.

[19] J. Høgsberg and S. Krenk, "Calibration of piezoelectric RL shunts with explicit residual mode correction," *Journal of Sound and Vibration*, vol. 386, pp. 65–81, 2017.

[20] W. Zhang, J. Li, H. Hao, and H. Ma, "Damage detection in bridge structures under moving loads with phase trajectory change of multi-type vibration measurements," *Mechanical Systems and Signal Processing*, vol. 87, pp. 410–425, 2017.

[21] W. Zuo, J. Bai, and J. Yu, "Sensitivity reanalysis of static displacement using taylor series expansion and combined approximate method," *Structural and Multidisciplinary Optimization*, vol. 53, no. 5, pp. 953–959, 2016.

[22] J. Guo, J. Jiao, K. Fujita, and I. Takewaki, "Damage identification for frame structures using vision-based measurement," *Engineering Structures*, vol. 199, Article ID 109634, 2019.

[23] Y. B. Yang, Y. C. Li, and K. C. Chang, "Constructing the mode shapes of a bridge from a passing vehicle: a theoretical study," *Smart Structures and Systems*, vol. 13, no. 5, pp. 797–819, 2014.

[24] D. Feng, M. Feng, E. Ozer, and Y. Fukuda, "A vision-based sensor for noncontact structural displacement measurement," *Sensors*, vol. 15, no. 7, pp. 16557–16575, 2015.

[25] E. J. OBrien and A. Malekjafarian, "A mode shape-based damage detection approach using laser measurement from a vehicle crossing a simply supported bridge," *Structural Control and Health Monitoring*, vol. 23, no. 10, pp. 1273–1286, 2016.

[26] W. Zhang, Z. Wang, and H. Ma, "Crack identification in stepped cantilever beam combining wavelet analysis with transform matrix," *Acta Mechanica Solida Sinica*, vol. 22, no. 4, pp. 360–368, 2009.

[27] D. G. Kasper, D. C. Swanson, and K. M. Reichard, "Higher-frequency wavenumber shift and frequency shift in a cracked, vibrating beam," *Journal of Sound and Vibration*, vol. 312, no. 1-2, pp. 1–18, 2008.

[28] E. Douka, S. Loutridis, and A. Trochidis, "Crack identification in beams using wavelet analysis," *International Journal of Solids and Structures*, vol. 40, no. 13-14, pp. 3557–3569, 2003.

[29] Y. Narkis, "Identification of crack location in vibrating simply supported beams," *Journal of Sound and Vibration*, vol. 172, no. 4, pp. 549–558, 1994.

[30] R. D. Cook, D. S. Malkus, M. E. Plesha, and R. J. Witt, *Concepts and Applications of Finite Element Analysis*, John Wiley & Sons, New York, NY, USA, 4th ed edition, 2002.